Structural Control of Poly(methyl methacrylate)-*g*-poly(dimethylsiloxane) Copolymers Using Controlled Radical Polymerization: Effect of the Molecular Structure on Morphology and Mechanical Properties

Hosei Shinoda[†] and Krzysztof Matyjaszewski*

Center for Macromolecular Engineering, Department of Chemistry, Carnegie Mellon University, 4400 Fifth Avenue, Pittsburgh, Pennsylvania 15213

Lidia Okrasa,[‡] Michal Mierzwa,[§] and Tadeusz Pakula*

Max Planck Institute for Polymer Research, Postfach 3148, 55021 Mainz, Germany

Received January 20, 2003; Revised Manuscript Received April 2, 2003

ABSTRACT: Atom transfer radical polymerization (ATRP), reversible addition−fragmentation chain transfer (RAFT) process, and the conventional radical polymerization (RP) were applied to the copolymerization of methyl methacrylate (MMA) and methacrylate-terminated poly(dimethylsiloxane) macromonomer (PDMS−MA). They resulted in PMMA-*g*-PDMS graft copolymers with various branching and molecular weight distributions. By applying appropriate conditions, ATRP led to homogeneously branched copolymer and RAFT to gradient branched copolymer. The RP process gave heterogeneously branched copolymer with large polydispersity. The structure and mechanical properties in these copolymers were analyzed.

Introduction

In the past several years, there was an explosion of papers on controlled/living radical polymerization (CRP)[1] such as atom transfer radical polymerization (ATRP),[2] nitroxide-mediated polymerization,[3] and degenerative transfer processes including the reversible addition−fragmentation chain transfer process (RAFT).[4] The reason for the extensive studies on CRP is because it can not only give polymers with predetermined molecular weight and narrow polydispersities but also provide (co)polymers with well-defined architectures (e.g., block, graft, brush, star, hyperbranched) from a wide range of readily available low-cost monomers. The precise control of polymer architecture allows to study and correlate the polymer molecular structure with many physical properties and overall morphology.

We will focus in this paper on graft copolymers.[5] Graft copolymers are already used for a variety of applications such as impact-resistant plastics, thermoplastic elastomers, compatibilizers, and polymeric emulsifiers. Since graft copolymers have many structural variables (comonomer composition, backbone length, branch length, spacing, spacing distribution, etc.), they have a great potential to realize new properties and/or improve performance of existing materials. One of the most useful ways to design and synthesize well-defined graft copolymers is the macromonomer method.[6,7]

Polymerization of poly(dimethylsiloxane) (PDMS) macromonomers to prepare organic/inorganic hybrid graft copolymers was already reported before.[8,9] PDMS is known as an inorganic polymer that shows unique properties such as low glass transition temperature, low surface energy, and high permeability of oxygen. For example, McGrath et al.[9] reported the free radical synthesis and characterization of the resulting poly(methyl methacrylate)-*g*-PDMS graft copolymer. The graft copolymers had both morphology and consequently bulk or surface properties dependent on its copolymer composition and branch length.

Recently, we demonstrated control over the distribution of branch spacing in the copolymerization of methacrylate-terminated PDMS macromonomer (PDMS−MA in Scheme 1) with methyl methacrylate (MMA) using CRP processes.[10,11] We showed the possibility of preparing different types of graft copolymers as illustrated in Scheme 2. While the copolymer F (prepared by free radical process) was heterogeneously branched, the copolymer A (prepared by ATRP) was more homogeneously branched. Copolymer R (prepared by RAFT) had a tapered structure, although it was intermolecularly homogeneous. We are interested in exploring how the structural differences would affect the mechanical properties of the obtained graft copolymers.

Three types of PMMA-*g*-PDMS graft copolymers of similar average molecular weight were prepared (M_n = 110 000 ± 20 000) with almost the same overall copolymer composition (∼50 wt % PDMS) and the same side chain length (M_n = 2370). They had, however, different polydispersities and different graft distributions to study a relationship between the polymer architectures and their properties.

Experimental Section

Synthesis and molecular characterization. A PDMS macromonomer with a methacrylate end group (PDMS−MA) was prepared according to the method reported elsewhere.[10] M_n = 2370; M_w/M_n = 1.25 (determined by GPC in toluene, polystyrene calibration). The functionality of terminal meth-

[†] Current address: Mitsui Chemicals, Inc., 580-32 Nagaura, Sodegaura City, Chiba 299-0265, Japan.

[‡] Current address: Department of Molecular Physics, Technical University of Lodz, Lodz, Poland.

[§] On a leave from Institute of Physics, Silesian University, Katowice, Poland.

* To whom correspondence should be addressed.

10.1021/ma034064g CCC: $25.00
Published on Web 06/03/2003

Scheme 1

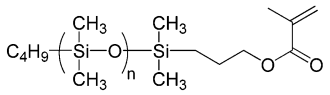

PDMS-macromonomer
(PDMS-MA)

Scheme 2

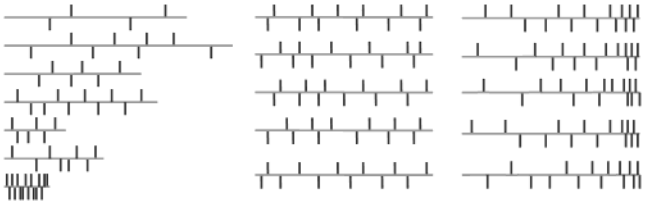

Polymer F **Polymer A** **Polymer R**

acrylate group $f = 1.0$ (^{1}H NMR spectroscopy). The detailed procedures for the copolymerizations and analysis were described previously.[11] All copolymerizations of PDMS−MA with MMA were conducted at a molar ratio $[PDMS-MA]_0/[MMA]_0 = 5/95$. ATRP was performed in xylene (35 wt %) at 90 °C using ethyl 2-bromoisobutyrate as initiator, CuCl as catalyst, and 4,4′-di-*n*-nonyl-2,2′-bipyridine (dnNbpy) as ligand with $[monomers]_0/[EBiB]_0/[CuCl]_0/[dnNbpy]_0 = 300/1/1/2$. RAFT was performed in xylene (31 wt %) at 60 °C using 2,2′-azobis(isobutyronitrile) (AIBN) as initiator and 2-phenyl-2-propyl dithiobenzoate (cumyl dithiobenzoate, CDB) as a RAFT agent with $[monomers]_0/[CDB]_0/[AIBN]_0 = 300/1/0.5$. The conventional free radical polymerization (FRP) was performed in xylene (40 wt %) at 75 °C using AIBN as initiator ($[monomers]_0/[AIBN]_0 = 400/1$). The conversion of MMA was measured by the gas chromatography. The conversion of PDMS−MA was determined by GPC measurements in toluene. The molecular weight of the graft copolymer was measured by GPC in tetrahydrofuran based on linear poly(methyl methacrylate) standards. The synthetic procedure and results are summarized in Table 1.

Characterization of structure and properties in bulk. Differential scanning calorimetry (DSC) measurements were performed using a Mettler DSC 30 apparatus at a temperature variation rate of 10 °C/min for both heating and cooling runs. The reported transition temperatures were determined from the second heating run. The glass transition temperature, T_g, was taken as the middle point of the dH/dt step in the DSC trace.

Small-angle X-ray scattering (SAXS) measurements were conducted using a rotating anode (Rigaku 18 kW) X-ray beam with a pinhole collimation and a two-dimensional detector (Simens) with 512 × 512 pixels. A double graphite monochromator for the Cu Kα radiation ($\lambda = 0.154$ nm) was used. The beam diameter was about 0.5 mm, and the sample-to-detector distance was 1.3 m. Measurements were performed at room temperature. The recorded scattered intensity distributions were integrated over the azimuthal angle and are presented as functions of the scattering vector ($s = 2 \sin \theta/\lambda$, where θ is the scattering angle).[12]

Dynamic mechanical measurements were performed by means of the Rheometrics RMS 800 mechanical spectrometer. Oscillatory shear deformation was applied under condition of controlled deformation amplitude which was changed with temperature between $\Delta\gamma = 0.0001$ at low temperatures and $\Delta\gamma = 0.05$ at high temperatures but always remaining in the range of the linear viscoelastic response of studied samples. Plate−plate geometry was used with plate diameters of 6 mm. The gap between plates (sample thickness) was about 1 mm. Experiments were performed under a dry nitrogen atmosphere. Results are presented as temperature dependencies of the storage (G') and loss (G'') shear modulus measured at a constant deformation frequency of 10 rad/s. The results below 50 °C were obtained under cooling with the rate 2 °C/min and above 50 °C under heating with the rate 2 °C/min.

Dielectric spectroscopy. Frequency- and temperature-dependent dielectric measurements were performed using the experimental setup of Novocontrol. The system was equipped with an Alpha high-resolution dielectric analyzer and temperature controller Quatro version 4.0. The complex dielectric modulus $M^*(\omega) = M'(\omega) - iM''(\omega)$ was determined in the frequency range from 10^{-2} to 3×10^6 Hz. Flat parallel plate capacitor (diameter 20 mm, thickness 0.06 mm) was used. The value of ac voltage applied to the capacitor was equal to 1 V. Temperature was controlled using a nitrogen gas cryostat, and the temperature stability of the sample was better than 0.1 K. Relaxation times have been determined from maximum positions in M'' ($\tau = 1/\omega_{max}$).

Cold drawing up to large deformations was performed for solution-cast films. The mechanical testing machine Instron 6000 was used. Samples having the thickness of 0.5 mm were drawn with the rate of 0.5/min at room temperature. The dependencies of nominal stress vs draw ratio were recorded. The materials showed similar behavior with the elastic deformation range at small strains, with the yield point indicating the beginning of plastic flow range and finally with a ductile fracture. The elastic modulus (E) and the coordinates of the yield point (λ_Y, σ_Y) as well as of the point of fracture (λ_B, σ_B) were determined as averages of 3−5 independent drawing experiments. The meaning of the parameters determined is illustrated in Figure 1.

The thick line represents average dependences. The parameters determined for these averaged curves are shown in Table 2.

Results and Discussion

To obtain three different architectures of PMMA-*g*-PDMS graft copolymers, three different methods (the conventional free radical polymerization (FRP, ATRP, and RAFT) were applied to the copolymerization of MMA and PDMS macromonomer (Table 1). The reactivity ratio of MMA r_{MMA} was estimated by the Jaacks[13] method:

$$r_{MMA} = k_{MMA^*/MMA}/k_{MMA^*/PDMS-MA}$$

The reactivity ratio is defined as the ratio of rate constants of addition of propagating PMMA radial to MMA vs PDMS macromonomer. The conditions for the preparation of these copolymers were different than earlier reported which also affected the overall reactivity ratios, which depend on the dilution and temperature.[10,11]

In the conventional free radical polymerization (FRP), r_{MMA} was 2.00 ± 0.02. The overall relative reactivity of the macromonomer was evaluated by the value $1/r_{MMA} = 0.5$. The overall reactivity of macromonomer is often lower than the inherent reactivity of the macromonomer based on the chemical structure of the terminal group.[7] One of the two additional factors that affect the reactivity is the diffusion control effect associated with the large size of the macromonomer.[14] The other factor is an incompatibility effect, potentially due to the thermodynamic repulsive interaction between a macromonomer and a propagating comonomer chain.[8] In the FRP process, the lowered reactivity of the macromonomer leads to the heterogeneously branched structure (copolymer F in Scheme 2). The copolymer generated at the early stage of the polymerization contains a small number of PDMS branches. Then, at the later stage, when the macromonomer dominates the residual comonomer pool, densely branched copolymers might be produced.

Table 1. Preparation of PMMA-*g*-PDMS Graft Copolymers by Radical Copolymerization of MMA and PDMS−MA[a]

polymer type	polymerization	r_{MMA}[e]	conversion, % MMA	conversion, % PDMS−MA	residual PDMS−MA,[f] wt %/copolymer[g]	M_n[f,h]	M_w/M_n[f,h]	molar ratio of PDMS/MMA in copolymer[f,i]
F	FRP[b]	2.00 ± 0.02	90	68	3	139 400	5.69	4.3/95.7
A	ATRP[c]	1.34 ± 0.03	80	79	1	86 000	1.58	4.5/95.5
R	RAFT[d]	1.70 ± 0.03	90	93	3	101 600	2.59	4.3/95.7

[a] PDMS−MA: $M_n = 2370$, $M_w/M_n = 1.25$, $F = 1.0$ $[PDMS-MA]_0/[MMA]_0 = 5/95$. After polymerization, obtained polymers were dissolved in acetone and reprecipitated from methanol. [b] PDMS−MA = 2.8 g, xylene = 40 wt %, $[monomers]_0/[AIBN]_0 = 400/1$, 75 °C, 5.5 h. [c] PDMS−MA = 2.8 g, xylene = 35 wt %, $[monomers]_0/[EBiB]_0/[CuCl]_0/[dnNbpy]_0 = 300/1/1/2$, 90 °C, 22 h. [d] PDMS−MA = 2.5 g, xylene = 31 wt %, $[monomers]_0/[CDB]_0/[AIBN]_0 = 300/1/0.5$, 60 °C, 34 h. [e] Calculated by the Jaacks method. [f] After reprecipitation. [g] Estimated from the peak intensity ration of PDMS−MA to copolymer in toluene−GPC. [h] Determined by THF−GPC against PMMA standard. [i] By ^{1}H NMR spectroscopy.

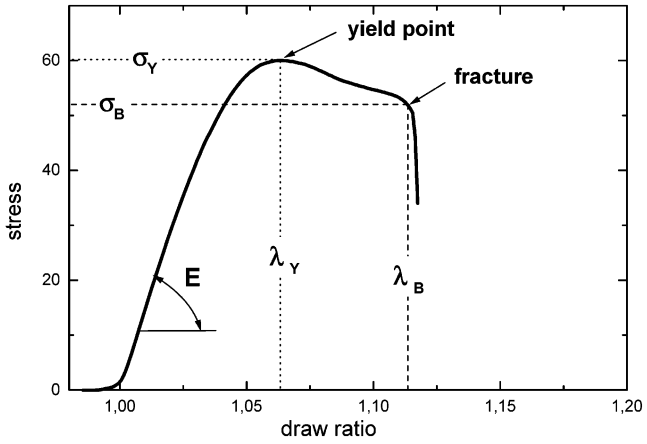

Figure 1. Schematic stress−strain dependence with the parameters characterizing the elasticity at small deformation as well as the yield and the break points.

Table 2. Some Parameters Characterizing Physical Properties of the Graft Copolymers

copolymer	T_g [°C] (DSC)	d [nm] (SAXS)	E [MPa][a]	σ_Y [MPa][a]	λ_Y[a]	σ_B [MPa][a]	λ_B[a]
FRP	−116.8	7.8	200			6.5	2.1
ATRP	−112.4	8.0	200	4.85	1.07	4.2	3.8
RAFT	−120.7	9.9	200	5.65	1.07	6.4	1.3

[a] Tensile test at room temperature.

The diffusion control effect becomes less important in CRP since the time interval of monomer addition to a polymer chain is much larger (seconds or minutes) than that in the conventional radical system (milliseconds).[15]

The r_{MMA} in ATRP system was 1.34 ± 0.03. In ATRP systems, the number of polymer chains is predetermined by the amount of initiator and, as observed in Figure 2, the chain length increased proportionally to the monomer conversion. In the absence of significant termination or transfer reactions, most of the growing chains remain active throughout the course of the polymerization. Therefore, when the reactivity of the macromonomer is close to that of a major comonomer, the branches will be constantly incorporated into all copolymer chains at a certain rate according to the macromonomer/comonomer composition in feed (copolymer A in Scheme 2). The narrow molecular weight distribution remained throughout the course of polymerization in ATRP (Figure 3).

Generally, the RAFT process can give similar r_{MMA} values and similar types of polymer architecture to the ATRP system.[11] However, since we intended to prepare the tapered branching or "toothbrush" type graft copolymer (copolymer R in Scheme 2), RAFT polymerization was intentionally conducted under such conditions

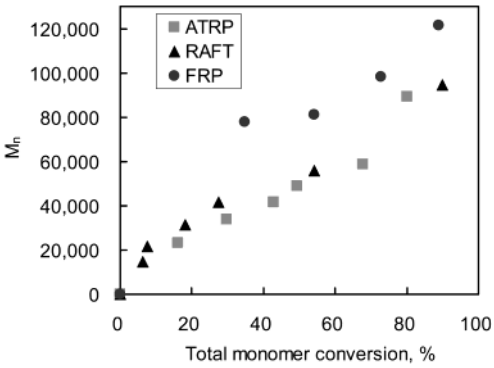

Figure 2. Dependence of molecular weight on conversion for the radical copolymerization of MMA and PDMS macromonomer (PDMS−MA, $M_n = 2370$, $M_w/M_n = 1.25$, $F = 1.0$). $[PDMS-MA]_0/[MMA]_0 = 5/95$. ATRP: $[monomers]_0/[EBiB]_0/[CuCl]_0/[dnNbpy]_0 = 300/1/1/2$, xylene = 35 wt %, 90 °C, N_2. RAFT: $[monomers]_0/[CDB]_0/[AIBN]_0 = 300/1/0.5$, xylene = 31 wt %, 60 °C, N_2. FRP: $[monomers]_0/[AIBN]_0 = 400/1$, xylene = 40 wt %, 75 °C, N_2. M_n was determined by THF−GPC.

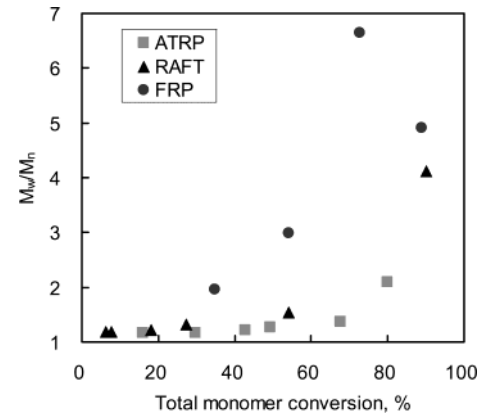

Figure 3. Dependence of polydispersity on conversion for the radical copolymerization of MMA and PDMS macromonomer (PDMS−MA, $M_n = 2370$, $M_w/M_n = 1.25$, $F = 1.0$). $[PDMS-MA]_0/[MMA]_0 = 5/95$. ATRP: $[monomers]_0/[EBiB]_0/[CuCl]_0/[dnNbpy]_0 = 300/1/1/2$, xylene = 35 wt %, 90 °C, N_2. RAFT: $[monomers]_0/[CDB]_0/[AIBN]_0 = 300/1/0.5$, xylene = 31 wt %, 60 °C, N_2. FRP: $[monomers]_0/[AIBN]_0 = 400/1$, xylene = 40 wt %, 75 °C, N_2. M_w/M_n was determined by THF−GPC.

that the reactivity of macromonomer was lower. By reducing the amount of solvent and lowering temperature, the obtained reactivity ratio r_{MMA} was 1.70 ± 0.04. Another factor could be the effect of the increased viscosity of the reaction mixture on the rate of addition−fragmentation chain transfer reaction. The molecular weight distribution at high conversion was rather broad for CRP. In an extreme case of RAFT, if this exchange reaction rate is slow, the control of the polymerization will be lost and become closer to the conventional radical polymerization.

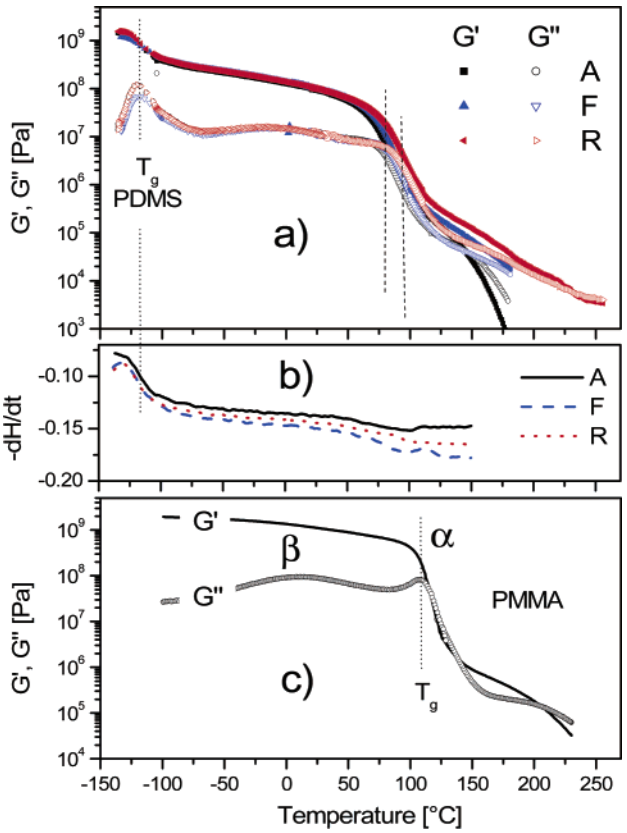

Figure 4. Temperature dependencies of the real (G') and imaginary (G'') parts of the shear modulus for (a) three PDMS copolymers with different architecture and for (c) a linear PMMA homopolymer sample with M_w = 101 000. (b) DSC heating runs (heating rate 10 K/min).

All copolymerization were conducted to high conversion (total monomers, 80−90%). Residual monomers were removed by reprecipitation from methanol. Obtained polymers F, A, and R had the same copolymer overall composition, the same branch length, and similar molecular weight, but different branch distributions and different polydispersities.

Trying to analyze the influence of differences in molecular structure of these grafted copolymers on the morphology and properties in bulk, the first question of interest was whether there is a microphase separation in these systems. Samples of bulk material were prepared by press-molding at 150 °C. DSC thermograms for all samples indicated features characteristic for a glass transition taking place within the temperature range in which the T_g of PDMS is usually observed (Figure 4b). Values of the observed T_g's are presented in Table 2. This was the first suggestion that in all systems there should be a phase or microphase, which preserves the bulk properties of a pure PDMS. The thermograms indicate also small steps just below 100 °C, which might be related to the glass transition in the backbone phase.

The presence of the low-temperature T_g was confirmed by the dynamic mechanical measurements performed with a constant deformation frequency (10 rad/s) within a broad temperature range. Results for the three samples are presented in Figure 4a. The glass transition of PDMS is indicated by the first drop in G' and the maximum in G'' at low temperatures, below −100 °C. The softening related to this transition is considerable and involves a drop of the real part of the shear modulus by almost 1 order of magnitude. There are only rather small differences in the mechanical behavior of the different samples in this temperature range, and this continues up to temperatures above the room temperature or even above 50 °C. Starting from this temperature, the second considerable softening takes place which should be attributed to a process which can be described as a glass transition in the phase, in which the PMMA backbone is the main component. The transition is broad, but related change of properties is so large that it should be considered as a main softening in these systems. The temperature range in which it takes place is considerably shifted to lower temperatures from the range characteristic for the glass transition in bulk PMMA. In Figure 4c the mechanical behavior of PMMA homopolymer is presented. A comparison with copolymer samples shows that the low-temperature features of PMMA, such as the β and α relaxations, are also present in the copolymer samples, however, broadened and shifted to lower temperatures. This can mean that the backbone phase is modified remarkably by more mobile components of the system such as some PDMS side chains or their aliphatic ends (see Scheme 1). The drop of shear modulus related to this main softening exceeds 2 orders of magnitude in G', and at temperatures above this transition the storage modulus levels off in the range of 10^5 Pa, which is characteristic for entangled or structured polymer melts. All this indicates that at least below the main softening transition (in the range including room temperature) all the studied systems are microphase-separated and behave macroscopically as thermoplastic elastomers.

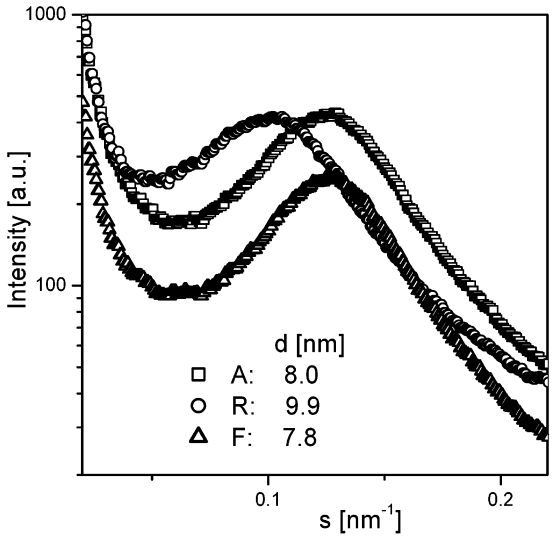

Figure 5. Small-angle X-ray scattering intensities recorded at room temperature for the three samples with various architectures.

To prove this, the small-angle X-ray scattering experiments were performed at room temperature, and the results are shown in Figure 5 in the form of scattered intensity vs the scattering vector *s*. The strong and clear intensity maxima detected for all samples indicate the microphase-separated states; however, the presence of only one broad peak excludes any long-range order and makes conclusions concerning type of order or identification of any specific morphological forms impossible. The irregularity of the supramolecular structure can result from a variable spacing of the grafts.[16] The correlation lengths related to the observed intensity

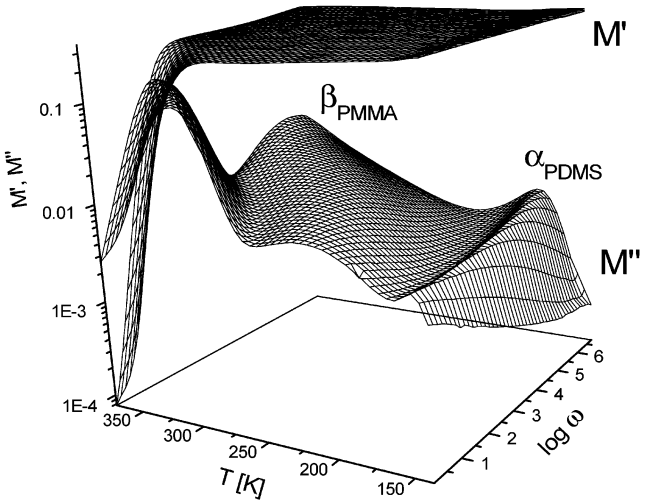

Figure 6. Frequency and temperature dependences of real and imaginary parts of the complex dielectric modulus for the copolymer A. The two relaxation processes are manifested by the maxima in M'' and are attributed to different phases.

maxima do not differ very much for various samples. For all of them the characteristic correlation lengths d are a little below 10 nm (see Table 2). The only longer correlation length in the copolymer R can result from the longer range heterogeneity related to the gradient in distribution of branches along chains which should involve composition gradients along the backbone like in the gradient copolymers. The weaker intensity of scattering in the copolymer F can be attributed to weaker structural correlations at all because of various types of structural heterogeneities. The most regular structure can be assigned to the copolymer A because of the high intensity related to the small correlation length controlled probably by sizes of the branches and relatively regular distances between them (see Scheme 2).

The above morphological differences may explain differences in mechanical behavior of the polymers seen above the main softening transition (Figure 4). For the copolymer A, the behavior in the melt suggests that homogenization takes place at higher temperatures. The typical short rubbery plateau is seen above the softening, which can be attributed to entanglements, and the system starts to flow at about 150 °C. There is a phenomenological similarity of this behavior to that presented for the PMMA homopolymer in Figure 4c. In contrast to that, the rubbery plateau in the other copolymer samples extends to considerably higher temperatures, which can be interpreted as a result of the persistent microphase-separated states. In the case of the copolymer R, for example, the elastic-like state seems to be observed up to temperatures higher than 220 °C. This behavior can be plausibly explained by the long-range ordering and microphase separation resulting from the compositional gradient along the backbone.

Additional proof of the assignment of relaxation processes in these samples was obtained from the dielectric spectroscopy. An example of the temperature and frequency dependencies of the complex dielectric modulus determined for the copolymer A is shown in Figure 6, in which the two relaxation processes—the α in the PDMS phase and the β in the PMMA-rich phase—are seen as maxima of M''.

Figure 7a shows a direct comparison of the temperature dependencies of the moduli determined by means

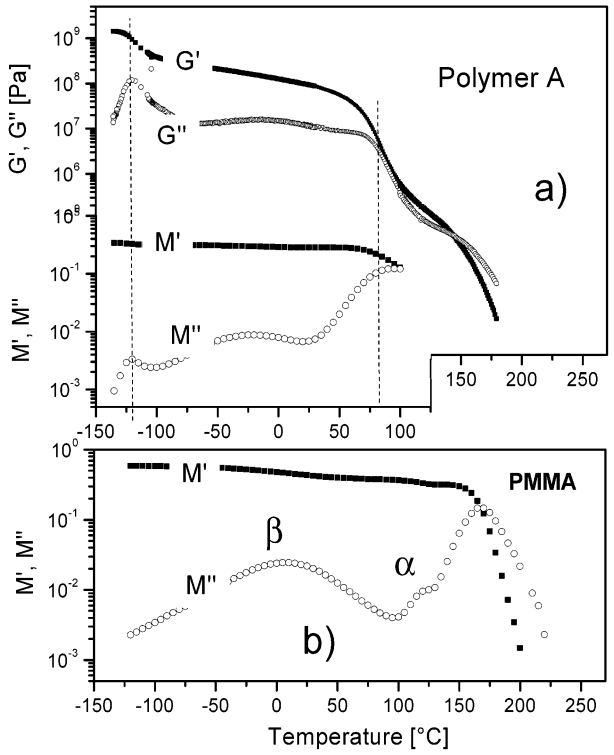

Figure 7. Comparison of temperature dependencies of the mechanical and dielectric module determined for (a) the grafted PDMS/MMA copolymer A and for (b) the linear PMMA homopolymer sample.

of both mechanical and dielectric methods. The low-temperature relaxation is detected by both methods and appears only because of the presence of the PDMS chains in the system. The broad relaxation observed in the temperature range between −50 and 50 °C is also seen in both mechanical and dielectric dependencies for the copolymer, but it is also observed in PMMA linear homopolymer melt (Figure 7b) where it is usually considered as β relaxation related to motion of the side groups. The α process in PMMA is overlapping with the conductivity peak, and it cannot be distinguished in the copolymer. Also, the dielectric spectra show that the relaxations characteristic of the PMMA fragments in the copolymers are shifted to lower temperatures with only small differences related to differences in the macromolecular architecture. The mechanical and dielectric measurements allow to determine the characteristic relaxation times and their temperature dependencies. An example of such dependencies is shown in Figure 8 for copolymer A. This map of the relaxations includes both dielectrically and mechanically determined results. Such a map together with the mechanical characteristics of this polymer shown in Figure 7a helps to recognize under which conditions (temperature and deformation rate) which properties of the material can be expected under small deformations.

The behavior of the copolymers in the range of large deformations was observed by recording stress−strain dependencies during cold drawing of solution-cast films at room temperature. The results obtained at a constant drawing rate are presented in Figure 9.

The dependencies are characteristic for thermoplastic elastomers when deformed in the range between the glass transitions of the constituents. They show an initial elastic range, a yield point followed by plastic flow range, which can be associated with a structural reori-

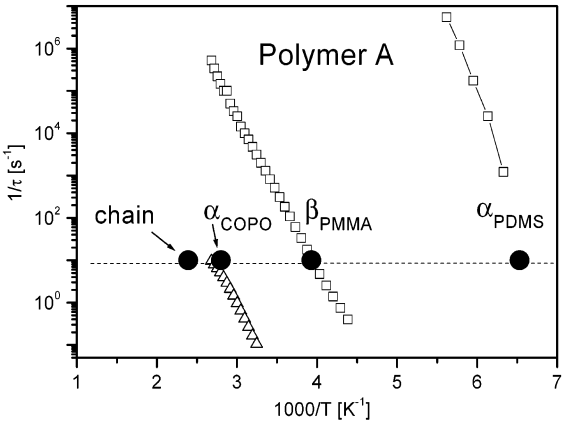

Figure 8. Comparison of relaxation times determined from the dielectrically determined spectra with these derived from the dynamic mechanical measurements.

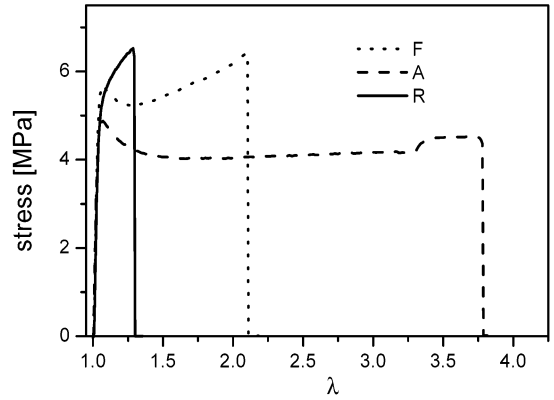

Figure 9. Stress−strain dependencies obtained by a cold drawing of the grafted copolymer films of various architectures. The dependencies are averages from three independent measurements performed under the same conditions.

entation and resulting strain hardening until a break takes place. Different than in the small deformation range, these results indicate considerable influence of polymer architectures on the properties. The parameters of the elastic range, of the yield point, and of the tensile strength (see Figure 1) are listed in Table 2. In agreement with the dynamic results, no differences in elastic modulus were observed. The highest stresses up to yielding are observed in the copolymer R in which the sample breaks when the yielding takes place. This seems to be in agreement with the conjectures based on the structural analysis presented above, suggesting that the microphase separation in this system accounts for the composition gradients along the polymers which results in segregation on the scale of whole macromolecules and can make the structural elements more resistant to stresses but breakable at low deformations because of specific concentrations of the ends of chains characteristic for diblock copolymer systems. Different behavior is observed for polymer A in which the uniformity of distributions of side chains along the backbone involves limits in lengths of unperturbed chain sequences, which can lead to reduction of the phase separation size scale. In consequence, this can reduce the thermal and mechanical stability of the microphase-separated state which under drawing can be detected as a low yield stress. On the other hand, more homogeneous structure can lead to more uniform plastic flow of the system which can cause the deformability up to $\lambda = 4$.

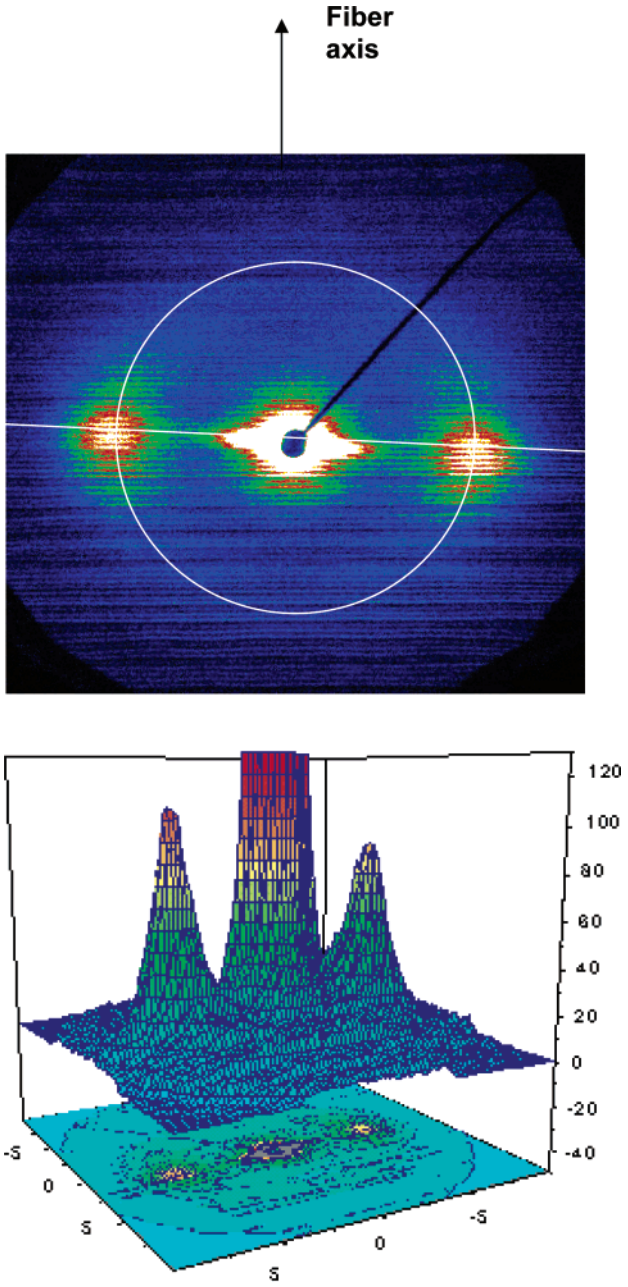

Figure 10. Small-angle X-ray scattering pattern of a melt drawn fiber from the copolymer A obtained by ATRP.

This uniformity of the A system was observed also in tests of spinability of melts performed for the copolymers. Whereas for melts of copolymers F and R, a drawing of fibers from the melt at approximately 150 °C was not successful because of breaking of the filaments at low deformations nice well-oriented fibers were obtained from the copolymer A. An example of the small-angle X-ray scattering pattern recorded for such a fiber is shown in Figure 10.

Conclusions

Different types of radical copolymerization of MMA and PDMS macromonomer under appropriate conditions gave different architectures of PMMA-*g*-PDMS graft copolymers. The copolymers obtained by CRP systems (ATRP and RAFT) had intermolecularly homogeneous branch structures with rather low polydispersity. The copolymer synthesized by ATRP had a homogeneous branch distribution. The copolymer prepared

by RAFT under certain conditions had a tapered branching structure. The conventional radical process gave heterogeneously branched structured copolymer with large polydispersity.

Different architectures displayed a weak influence on the relaxation spectra controlling the properties at small deformations. Some differences in the morphologies and in the stabilities of the microphase-separated states were detected which involved large differences in mechanical properties at large deformations.

Different characteristic size scales of the microphase separation in polymers with a homogeneous and with a gradient like distribution of grafted side chains are suggested as influencing the behavior at large deformations and a flow of the graft copolymers.

Acknowledgment. Financial support from the National Science Foundation (DMR 00-90409) and industrial members of the Controlled Radical Polymerization Consortium at Carnegie Mellon University are greatly acknowledged. H.S. acknowledges financial support from Mitsui Chemicals, Inc. L.O. acknowledges support by a Marie Curie Fellowship of the European Community Program "Improving Human Research Potential and the Socio-economic Knowledge Base" under Contract HPMF-CT-2000-00731.

References and Notes

(1) Matyjaszewski, K., Ed. *Controlled Radical Polymerization*; ACS Symp. Ser. Vol. 685; American Chemical Society: Washington, DC, 1998. Matyjaszewski, K., Ed. *Controlled/Living Radical Polymerization: Progress in ATRP, NMP, and RAFT*; ACS Symp. Ser. Vol. 768; American Chemical Society: Washington, DC, 2000. Matyjaszewski, K.; Davis, T. P. *Handbook of Radical Polymerization*; Wiley-Interscience: Hoboken, 2002. Matyjaszewski, K., Ed. *Advances in Controlled/Living Radical Polymerization*; ACS Symp. Ser. Vol. 854; American Chemical Society: Washington, DC, 2003.

(2) Wang, J. S.; Matyjaszewski, K. *J. Am. Chem. Soc.* **1995**, *117*, 5614. Wang, J.-S.; Matyjaszewski, K. *Macromolecules* **1995**, *28*, 7901. Patten, T. E.; Xia, J.; Abernathy, T.; Matyjaszewski, K. *Science* **1996**, *272*, 866. Patten, T. E.; Matyjaszewski, K. *Adv. Mater.* **1998**, *10*, 901. Patten, T. E.; Matyjaszewski, K. *Acc. Chem. Res.* **1999**, *32*, 895. Matyjaszewski, K. *Chem.—Eur. J.* **1999**, *5*, 3095. Matyjaszewski, K.; Xia, J. *Chem. Rev.* **2001**, *101*, 2921. Kamigaito, M.; Ando, T.; Sawamoto, M. *Chem. Rev.* **2001**, *101*, 3689.

(3) Solomon, D. H.; Rizzardo, E.; Cacioli, P. U.S. Pat. 4,581,429, 1986. Georges, M. K.; Veregin, R. P. N.; Kazmaier, P. M.; Hamer, G. K. *Trends Polym. Sci.* **1994**, *2*, 66. Greszta, D.; Matyjaszewski, K. *Macromolecules* **1996**, *29*, 7661. Benoit, D.; Grimaldi, S.; Robin, S.; Finet, J.-P.; Tordo, P.; Gnanou, Y. *J. Am. Chem. Soc.* **2000**, *122*, 5929. Hawker, C. J.; Bosman, A. W.; Harth, E. *Chem. Rev.* **2001**, *101*, 3661.

(4) Gaynor, S.; Wang, J. S.; Matyjaszewski, K. *Macromolecules* **1995**, *28*, 8051. Chiefari, J.; Chong, Y. K. B.; Ercole, F.; Krstina, J.; Jeffery, J.; Le, T. P. T.; Mayadunne, R. T. A.; Meijs, G. F.; Moad, C. L.; Moad, G.; Rizzardo, E.; Thang, S. H. *Macromolecules* **1998**, *31*, 5559. Moad, G.; Chiefari, J.; Chong, Y. K.; Krstina, J.; Mayadunne, R. T. A.; Postma, A.; Rizzardo, E.; Thang, S. H. *Polym. Int.* **2000**, *49*, 993.

(5) Borner, H. G.; Matyjaszewski, K. *Macromol. Symp.* **2002**, *177*, 1.

(6) Schulz, G. O.; Milkovich, R. *J. Appl. Polym. Sci.* **1982**, *27*, 4773.

(7) Meijs, G. F.; Rizzardo, E. *J. Macromol. Sci., Rev. Macromol. Chem. Phys.* **1990**, *C30*, 305.

(8) Tsukahara, Y.; Hayashi, N.; Jiang, X.-L.; Yamashita, Y. *Polym. J.* **1989**, *21*, 377.

(9) Smith, S. D.; DeSimone, J. M.; Huang, H. Y. G.; Dwight, D. W.; Wilkes, G. L.; McGrath, J. E. *Macromolecules* **1992**, *25*, 2575.

(10) Shinoda, H.; Miller, P. J.; Matyjaszewski, K. *Macromolecules* **2001**, *34*, 3186.

(11) Shinoda, H.; Matyjaszewski, K. *Macromol. Rapid Commun.* **2001**, *22*, 1176.

(12) Guinier, A. *X-Ray Diffraction in Crystals, Imperfect Crystals and Amorphous Bodies*; W.H. Freeman & Co.: San Francisco, 1963.

(13) Jaacks, V. *Makromol. Chem.* **1972**, *161*, 161.

(14) Radke, W.; Mueller, A. H. E. *Makromol. Chem., Macromol. Symp.* **1992**, *54*, 583. Morawetz, H.; Cho, J. R.; Gans, P. J. *Macromolecules* **1973**, *6*, 625.

(15) Roos, S. G.; Mueller, A. H. E.; Matyjaszewski, K. *Macromolecules* **1999**, *32*, 8331. Shinoda, H.; Matyjaszewski, K. *Macromolecules* **2001**, *34*, 6243.

(16) Pochan, D. J.; Guido, S. P.; Pispas, S.; Mays, J. W.; Ryan, A. J.; Fairclough, J. P. A.; Hamley, I. W.; Terrill, N. J. *Macromolecules* **1996**, *29*, 5091. Ge, S.; Guo, L.; Rafailovotch, M. H.; Sokolov, J.; Peiffer, D. G.; Schwartz, S. A.; Colby, R. H.; Dozier, W. D. *Langmuir* **1999**, *15*, 2911.

MA034064G